Science
AAAS

Supplementary Materials for

Structure of a trapped radical transfer pathway within a ribonucleotide reductase holocomplex

Authors: Gyunghoon Kang, Alexander T. Taguchi, JoAnne Stubbe, and Catherine L. Drennan

Correspondence to: stubbe@mit.edu, cdrennan@mit.edu

This PDF file includes:

Protein preparation

α2 and E52Q/F_3Y-β2 were prepared as previously described (*9*). The concentrations of α2 and E52Q/F_3Y-β2 were determined using their extinction coefficients (A280) of 189 and 131 $mM^{-1}cm^{-1}$, respectively. All concentrations are for the respective dimers. α2 had a specific activity for the GDP/TTP pair of ~1500 nmol/min/mg as determined by a coupled spectrophotometric assay (*33*). E52Q/F_3Y-β2 is active under single-turnover conditions and has a radical content of 0.8-0.9 radical/dimer (*9*).

dGDP formation with pre-reduced α2 and E52Q/F3Y122•-β2

Pre-reduced α2 was generated with α2 protein (specific activity 2200 nmol/min/mg using CDP/ATP substrate/effector pairs) in 50 mM HEPES pH 7.6, 5% glycerol, 1 mM TCEP. α2 was incubated with final concentration of 20 mM hydroxyurea for 5 min at 25°C. α2 was desalted on a PD10 (Sephadex G25 Column, CV = 10 mL) into 50 mM HEPES pH 7.6 (*31*).

The reaction mixture contained 20 μM pre-reduced WT-α2, 20 μM E52Q/F_3Y122•-β2 (0.8-0.9 Y•/β2), 50 μM TTP, 50 mM HEPES pH 7.6, 15 mM $MgSO_4$, 1 mM EDTA. The reaction was initiated by [^{3}H]GDP (250 μM, 18154 cpm/nmol, Perkin Elmer) at 25 °C. At defined time points, 30 μL were withdrawn and quenched in 25 μL 2% (v/v) perchloric acid and incubated on ice. At the end of the time point, the quenched mixture was spun down (25,000 g x 10 min 4°C) and 50 μL of supernatant was transferred to a new centrifuge tube. The supernatant mixtures were neutralized with 7 μL cold 2 M KOH. The quenched and neutralized time point samples were frozen to precipitate potassium perchlorate. The samples were then thawed on ice and spun down for 10 min (25,000 g, 4°C). 50 μL of each supernatant was transferred to a 1.5-mL screw-top microfuge tube, and 20 units of calf-intestine alkaline phosphatase (Roche) were added to give a final volume of 120 μL with a final concentration of 50 mM Tris, 1 mM EDTA (pH 8.5). The samples were incubated at 37 °C for 2 h, and then heated at 95°C for 5 min and spun down for 10 min at 25,000 g. These samples were analyzed by a Waters 2480 HPLC with an Altech Adsorbosphere nucleotide nucleoside C-18 column (250 mm x 4.6 mm, 7 μm) at a flow rate of 2 mL/min. 50 μL of sample was injected and eluted with a linear gradient of 0 – 6 % methanol over 25 min. Fractions (1 mL) were collected and 600 μL of each was analyzed for the amount of dG by scintillation counting.

Radical quantification of pre-reduced α2 and E52Q/F3Y122•-β2

20 μM α2 was mixed with 1 mM GDP and 0.25 mM TTP in 50 mM HEPES, 15 mM $MgSO_4$, and 1 mM EDTA and incubated for 50 s in a 25 °C water bath. The reaction was initiated by the addition of 20 μM E52Q/2,3,5-F_3Y122-β2. The total volume was 220 μL. The reaction was incubated at 25 °C for 13, 20, 30, 40, 60, 120, 180 s and frozen in an isopentane bath cooled by liquid nitrogen. The EPR spectra were collected at 77 K on a Bruker EMX X-band spectrometer equipped with a liquid helium cryostat. The spectra were measured with microwave frequency 9.37 GHz, power 63 mW, modulation amplitude 1.5 G, modulation frequency 100 kHz, scan time 30 s. The 2,3,5-F_3Y122 radical was subtracted based on F hyperfine from the low field region.

Cryo-EM grid preparation used for data collection

Grids were prepared on Quantifoil 1.2-1.3 Cu 300 mesh holey-carbon grids and plunged on a Thermo Fisher Scientific Vitrobot (Mk IV) cryo-plunger. The final protein solution contained 0.8 μM α2, 1.6 μM β2, 0.2 mM TTP, 1 mM GDP, 50 mM HEPES, 15 mM $MgSO_4$, 1 mM EDTA, 25 mM NaAcetate, pH 7.6. Before applying to the grid, α2 was incubated with nucleotides for 1 min at room temperature and then the reaction was initiated by addition of β2. Excess β2 was used to maximize complex formation. Addition of NaAcetate was determined to alleviate issues of particle aggregation that was observed during the grid-screening stage. The final solution was incubated for an additional 50 sec at room temperature before application to grid. Grids were glow-discharged at -15 mA for 1 min (PELCO easiGlow) before protein solution was applied. 3.2 μL sample was applied to the grids that were blotted for 4.5-5 s (Whatman filter paper #1) before plunging into liquid ethane and transferring to storage grids. The temperature and humidity inside the Vitrobot chamber were set to 10°C and 90%, respectively.

Data collection of cryo-EM data

Data were collected at the Cryo-EM Core Facility at the University of Massachusetts Medical School at Worcester on a Thermo Fisher Titan Krios 300 kV electron microscope equipped with a Gatan GIF K2 camera across two collections. Both data collections had identical collection parameters and both were from the same preparation of protein. Parameters were as follows: 1.05 Å/pix (collected at super-resolution of 0.529 Å/pix), 30 frames, 1.57 $e^-/Å^2$/frame dose, defocus range 1.3-2.8 μm. The two data sets contained 3926 and 2312 movies, respectively. These parameters are summarized in **Table S3**.

Frame alignment, defocus estimation, and micrograph assessment in SPHIRE

Individual frames of each dose-fractionated exposure were aligned and summed using motion_cor2 (*34*), and the defocus of the summed frames were estimated using CTER (*35*). The outputs of the motion_cor2 and CTER were used to perform CTF and drift assessments within the SPHIRE software suite (*36*). The overall average drift after discarding outliers was 5.92 Å total, and the defocus cut-off was set to 3.58 um. Based on these criteria, the two data sets containing 3926 and 2312 movies were truncated to 2946 and 2116 movies, respectively, for a total of 5062 micrographs used for selection moving forward.

Particle selection

An initial set of ~2000 particles were manually picked from a subset of aligned movies. These model particles were then used to train a neural-net automated particle picker Topaz (*37*), which was then used to automatically pick particles from the entire data set using a threshold of -2 for the cut-off for positive signal, which resulted in 200220 initial particle hits.

Frame alignment and defocus estimation in Relion 3.0

Frame alignment was rerun using Relion's implementation of motion_cor2 within the Relion 3.0 software suite (*38*). CTF estimation was also rerun using the output from Relion's motion_cor2 using ctffind4 (*39*).

Map generation and refinement in Relion 3.0

The coordinate set of 200220 particles from Topaz was used to re-extract particles (box-size 240 pix) and perform initial reference-free 2D classification (mask diameter 180 Å) to generate 1000 2D class averages. Classes corresponding to α2β2 vs α2 were readily distinguishable by observation (Fig. S14), therefore, 68 total classes, comprising 80386 α2β2 particles were sub-selected for further analysis. These 68 classes were used to generate a *de novo* initial reference-free 3D model using no imposed symmetry (i.e. C1). This step was followed by high-resolution 3D refinement using the entire particle set. Unsupervised 3D classification did not yield additional classes nor improve resolution so the entire particle set (80386 particles) was taken for further analysis. Map sharpening was performed in Relion ("post-processing") with a mask generated with a low pass filter of 15 Å, initial binarization threshold of 0.0043, binary map extended by 6 pix, with a soft edge of 6 pix. CTF refinement was performed using CTF parameter fitting and per-particle defocus fitting flagged. Particle polishing was performed using the Bayesian method of particle motion estimation in Relion. The refined particle set was used to rerun high-resolution 3D refinement with the aforementioned mask to generate the final map. The final resolution at FSC=0.143 was 3.6 Å and local resolution was estimated using the ResMap (1.1.4) (*40*) executable within the Relion 3.0 GUI.

Model building and refinement

Coordinates from the crystal structure of inhibited class Ia RNR from *E. coli* (PDB 5CNV) were docked into the EM reconstruction using UCSF ChimeraX and used as the starting model (*13, 41*). Iterative rounds of model building and refinement were done using Coot (*42*) and Phenix Real Space Refine (*43*), respectively. For real space refinement, resolution was set to 3.2 Å, and electron scattering table was selected. Model quality was evaluated using Molprobity (*44*) and EMRinger (*45*). The final model fits the map well and contains residues 1-736 (of 761) of α chain A, 5-742 (of 761) of α chain B, 1-375 (of 375) β chain C, 1-341 (of 375) β chain D. Figures of the model and map were generated using UCSF ChimeraX. Coot, Phenix, and ChimeraX were licensed through the SBGrid Consortium operated out of Harvard Medical School (*46*). Refinement and model statistics are summarized in **Table S4**.

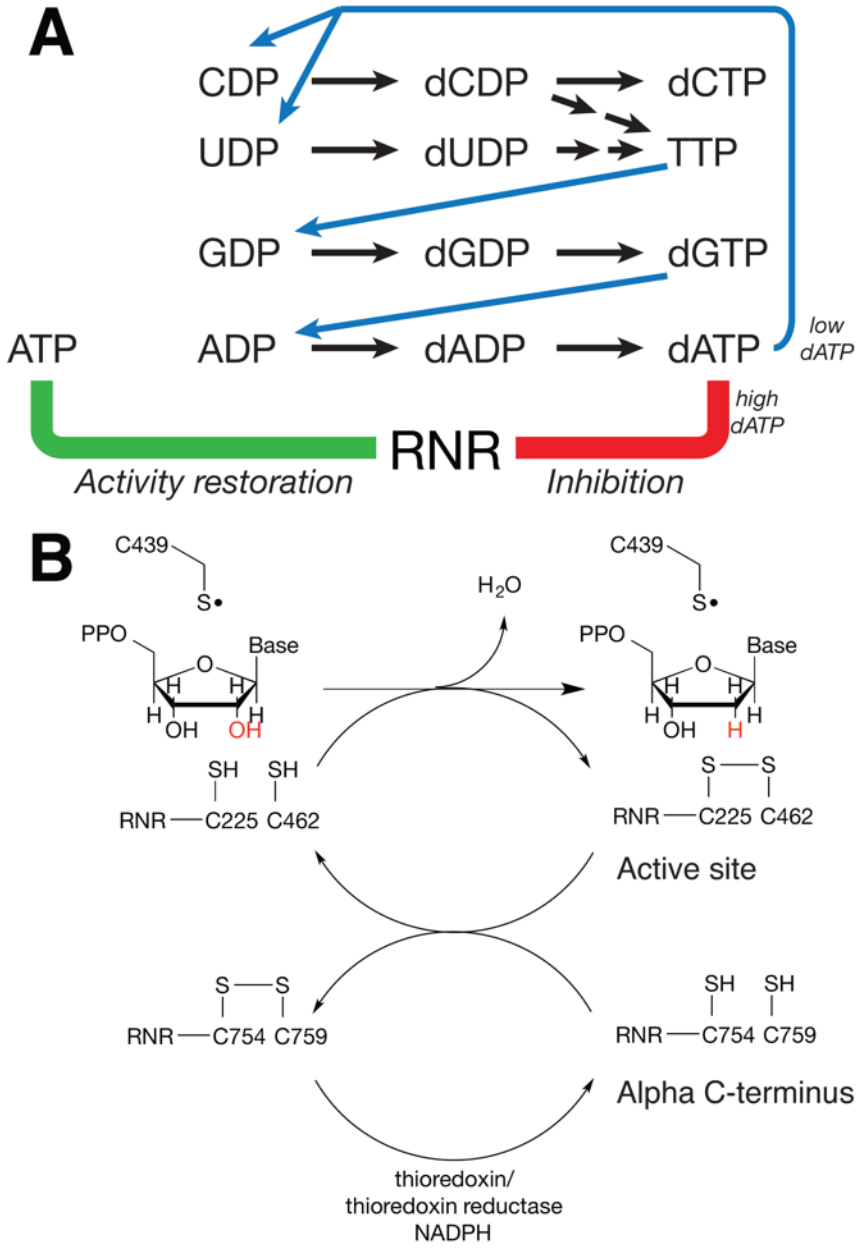

Fig. S1: RNR reduces all four ribonucleotide substrates and is allosterically regulated. A) Substrate specificity is regulated allosterically via the binding of deoxynucleotides. Under low concentrations of dATP, CDP and UDP reduction is favored. TTP in turn leads to GDP reduction and dGTP leads to ADP reduction. When the concentration of dATP increases, it can bind to a second allosteric site, the activity site, which inhibits enzymatic activity. ATP can compete for binding at this activity site to restore activity (*14, 47*). B) Enzymatic turnover in class Ia RNR involves a series of redox-active cysteine pairs. The reducing equivalents for nucleotide reduction is initially provided by a pair of cysteines (C225/462) in the active site that get oxidized to form a disulfide concomitant with product formation. This disulfide gets reduced by a second pair of redox-active cysteines (C754/759) found at the C-terminus of the α subunit. Ultimately, the disulfide between C754 and C759 gets reduced via the thioredoxin/thioredoxin reductase pair together with NADPH, thus allowing for additional rounds of turnover.

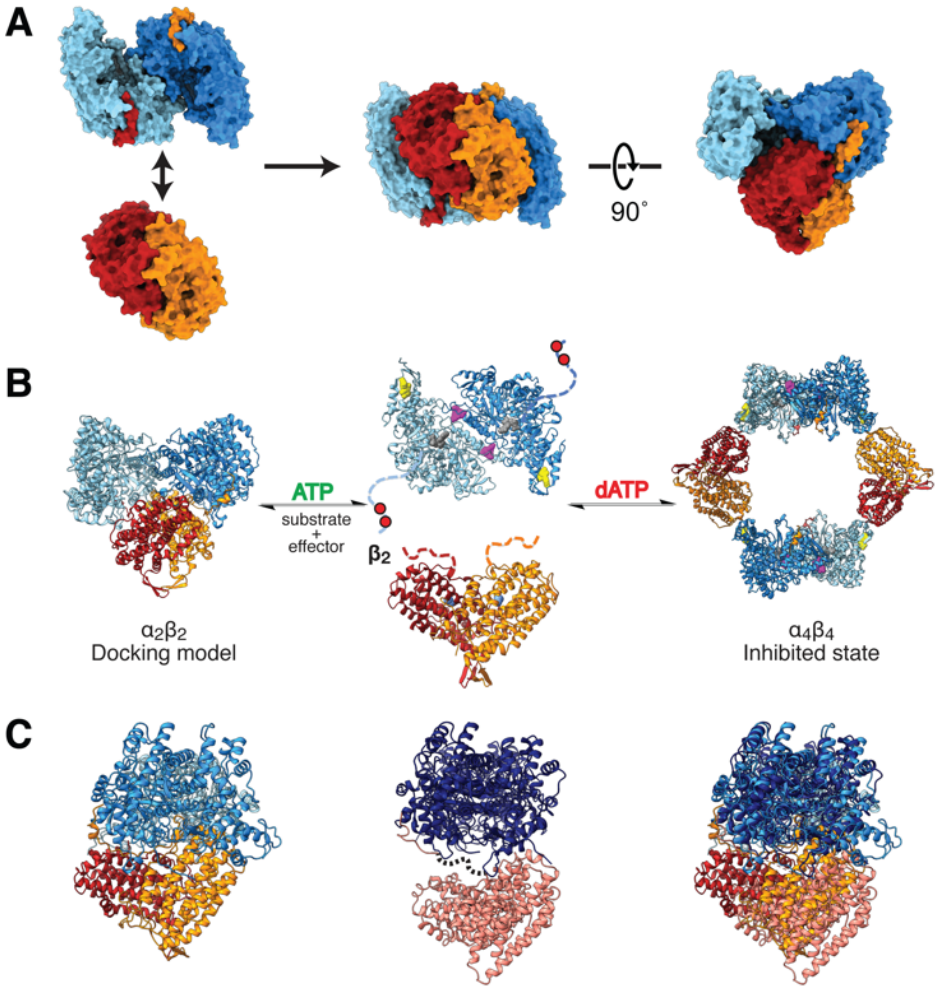

Fig. S2: Class I RNRs are structurally dynamic. A) The α2β2 docking model for *E. coli* class Ia RNR was proposed based on shape complementarity along the 2-fold symmetry axes of the α2 and β2 crystal structures (*5*). B) *E. coli* class Ia RNR is composed of two homodimeric subunits. α2, shown in cyan/blue, houses the active site (substrate shown in grey spheres) and two allosteric nucleotide-binding sites (effectors shown in yellow and purple spheres), and β2, shown in red/orange, houses the diferric tyrosyl radical cofactor (dark-blue spheres). dATP binding to the N-terminal cone domain of α2 generates the inhibited α4β4 state and dATP displacement by ATP can shift the equilibrium towards the active α2β2 state, shown above as the symmetric docking model. Crystal structures of both α2 and β2 have disordered C-terminal tails (shown as dotted lines of corresponding color) that play essential roles in catalysis. The red circles correspond to C754/C759 discussed in Fig. S1B. The position of the last ~15 residues of β, proposed from previous crystal structures, are shown on α2 in red/orange. Colors are as in previous panel with structures shown in surface representation. C) Dynamics of interface formation. Previously reported holoRNR complex from the class Ib RNR from *Salmonella typhimurium* (middle, PDB: 2BQ1 (*11*)) showed an open interface between α2 (dark blue) and β2 (pink) and residues of the PCET pathway disordered (black dashed line). Cryo-EM structure described in this work (left) shows a closed interface between α2 (cyan/blue) and β2 (orange/red), with an intact PCET pathway. Right shows an overlay of the two structures aligned to their respective α2 subunits.

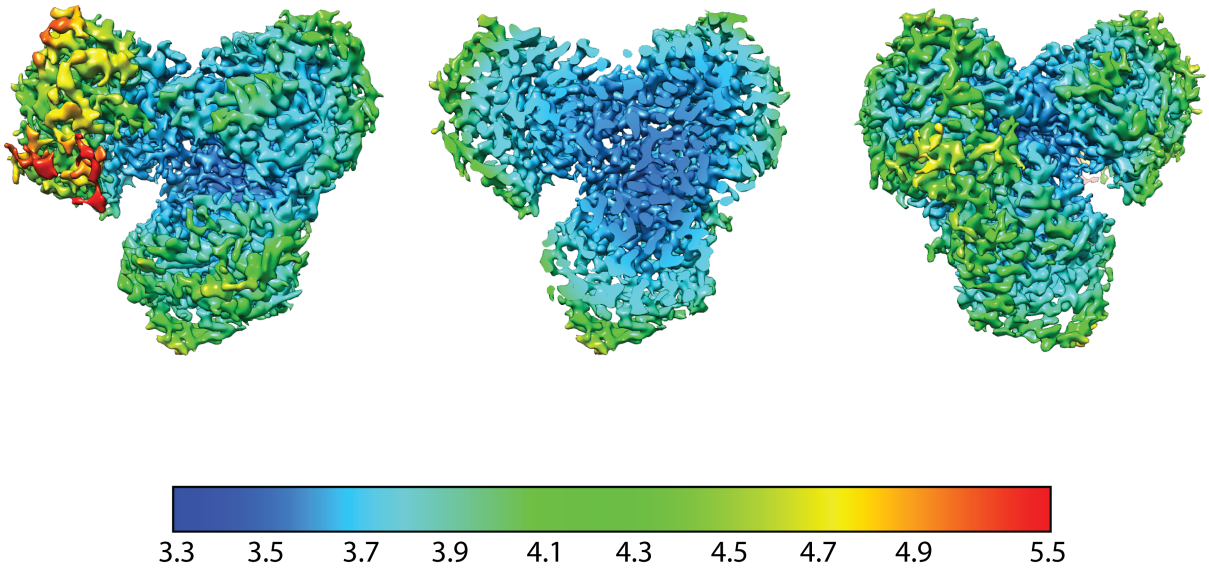

Fig. S3: Local resolution maps of cryo-EM density as calculated using the link to ResMap (*40*) through Relion (*38*). Left: Local resolution map of final 3D refinement. The resolution ranges from 3.3 Å within the core of the complex, including at the α2-β2 interface, to 5.5 Å at the N-terminus of one of the α monomers (α′). Middle: Cross-section view to highlight that the highest resolution region is found within the core of the complex, including the α2-β2 interface. Right: 180° rotation of the orientation shown on the far left (i.e. the backside). Resolution scale is as shown and is in Å. Disordered regions are summarized in Table S1 and range of B-factors are summarized in Table S4.

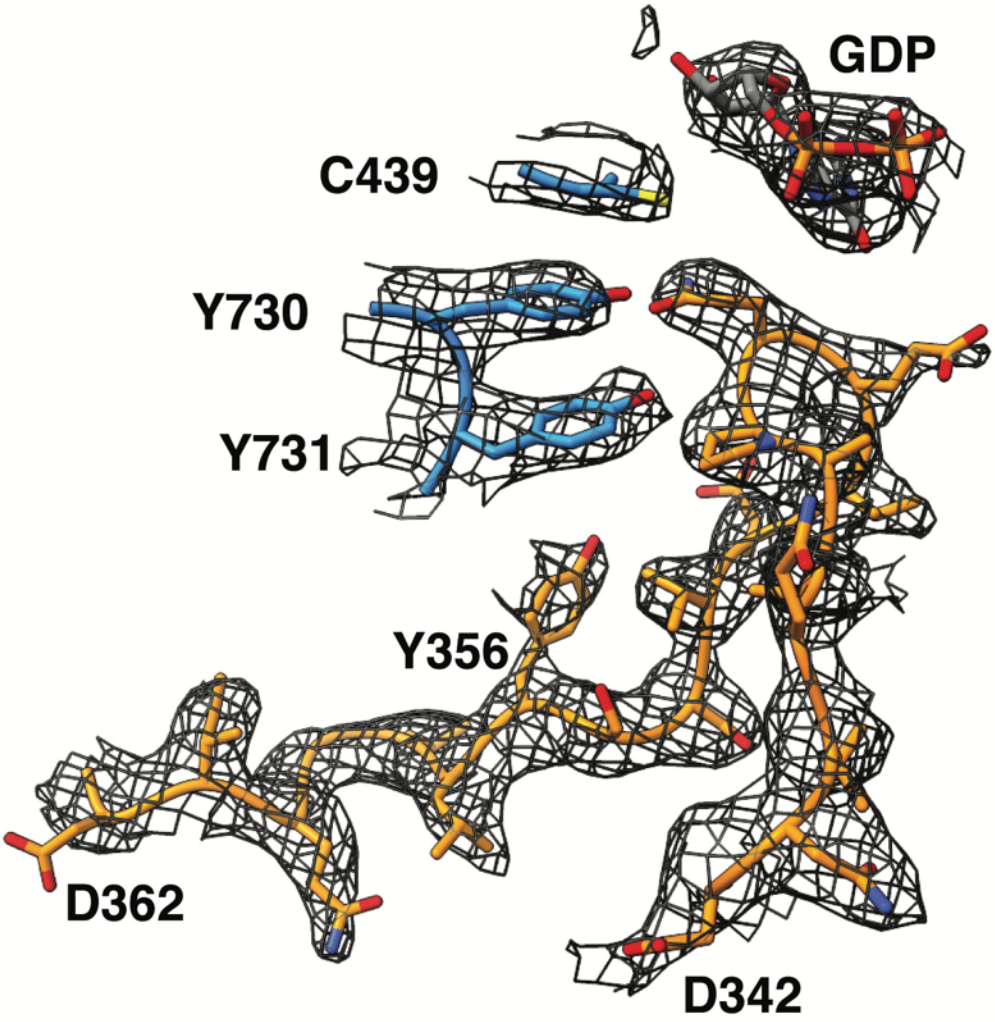

Fig. S4: Representative density in region of highest resolution at the α2-β2 interface. Shown here are newly modeled residues 342-362 of β (as shown in **Fig. 2**) in the context of key residues C439, Y731, Y730, and substrate GDP of α. α residues are shown in blue, β residues in orange and carbons of substrate GDP in grey. Density threshold set to 0.0249.

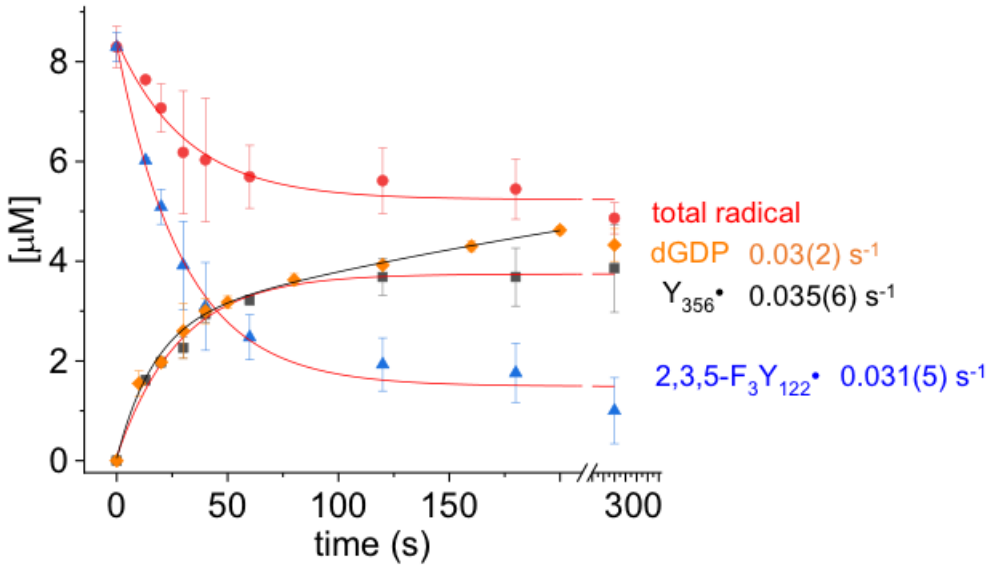

Fig. S5: Monitoring dGDP formation and radical content of WT-α2 (20 μM) and E52Q/trifluorotyrosine122(F_3Y122)-β2 (20 μM) in the presence of substrate GDP and specificity effector TTP. A fast phase, in which we observe approximately one-half equivalents of product dGDP form, occurs within the first ~50-60 seconds following reaction initiation, followed by a slow phase where we observe continued formation of dGDP. Approximately 25% of total radical is lost during the fast phase as well as ~75% of F_3Y122•. All data are representative of two independent experiments.

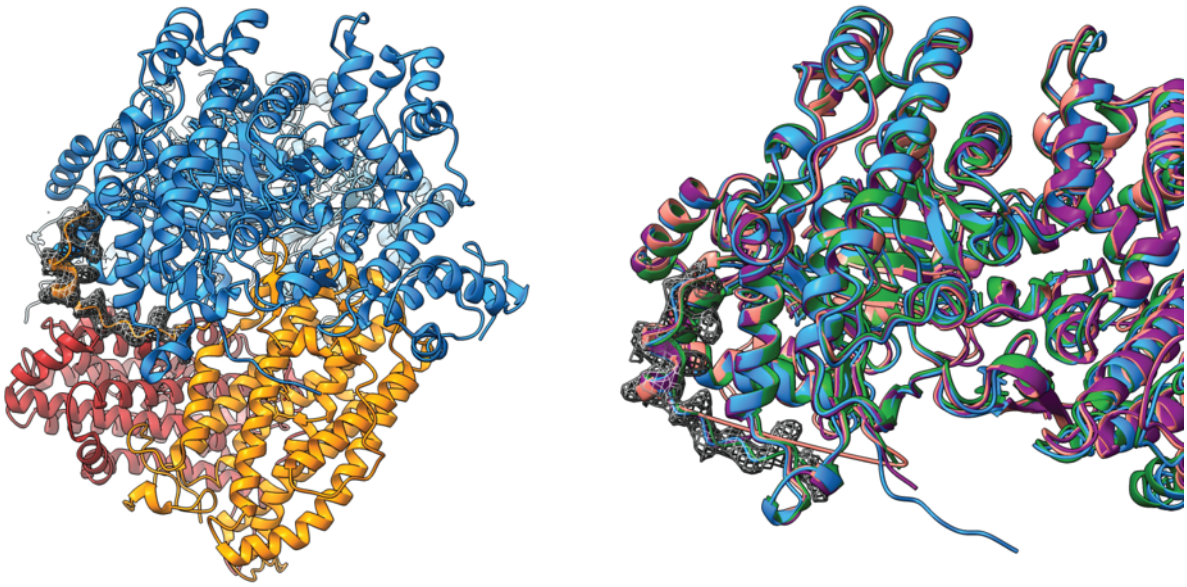

Fig. S6: Binding site of C-terminus of the β subunit on the α subunit is consistent with previous crystal structures. Left: In our structure, the C-terminus of β binds to a cleft formed by two alpha-helices of the α subunit (*5*) (Fig. S2). Cryo-EM density corresponding to residues 360-375 of β is shown in grey mesh. Colors are as in Fig. 1C. Right: Superposition of three crystal structures showing that the position of the C-terminus of β is consistent. The pink (PDB: 1RLR (*5*)) and purple (PDB: 2R1R (*14*)) structures correspond to apo-α and TTP-bound-α, respectively, where a peptide mimic of the β C-terminus was added to the crystallization conditions. The green structure corresponds to the inhibited structure of α4β4 with GDP/TTP bound (PDB: 5CNV (*13*)), where the last 16 residues of β were found ordered along this cleft in α. Our structure of α2β2 is in blue.

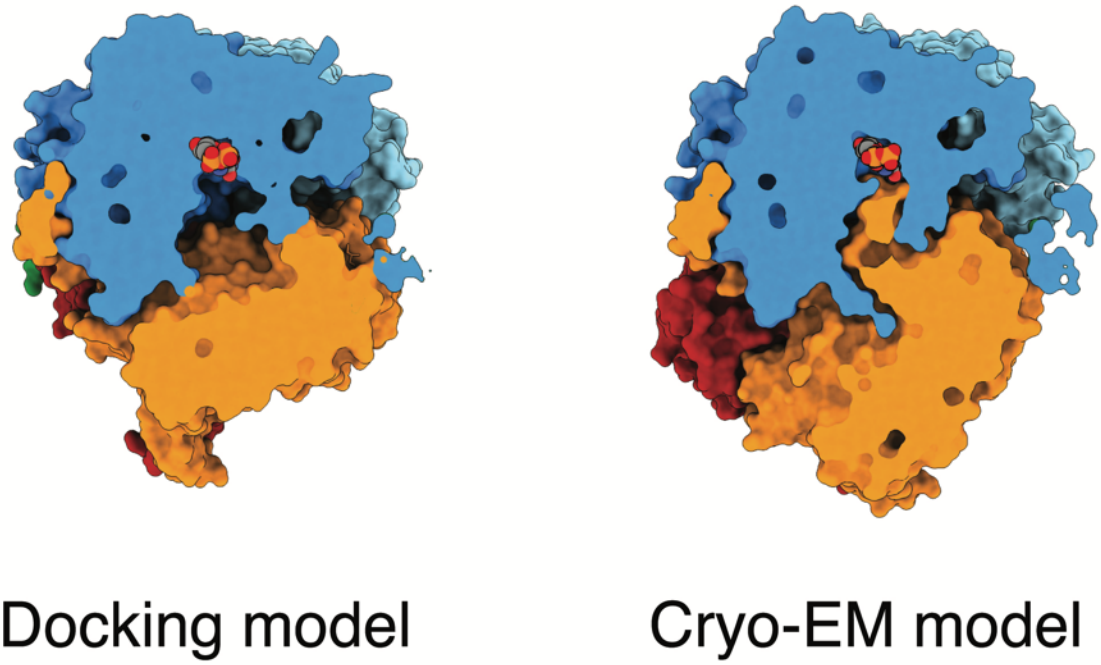

Fig. S7: Comparison of packing of active site between docking model and Cryo-EM structure. A slice through a surface representation of the docking model (left) reveals a large cavity around the substrate and active site. A slice through a surface representation of the cryo-EM model (right) shows that β (orange) packs in very tightly into the active site of α (blue), blocking solvent accessibility. Substrate GDP is shown in spheres.

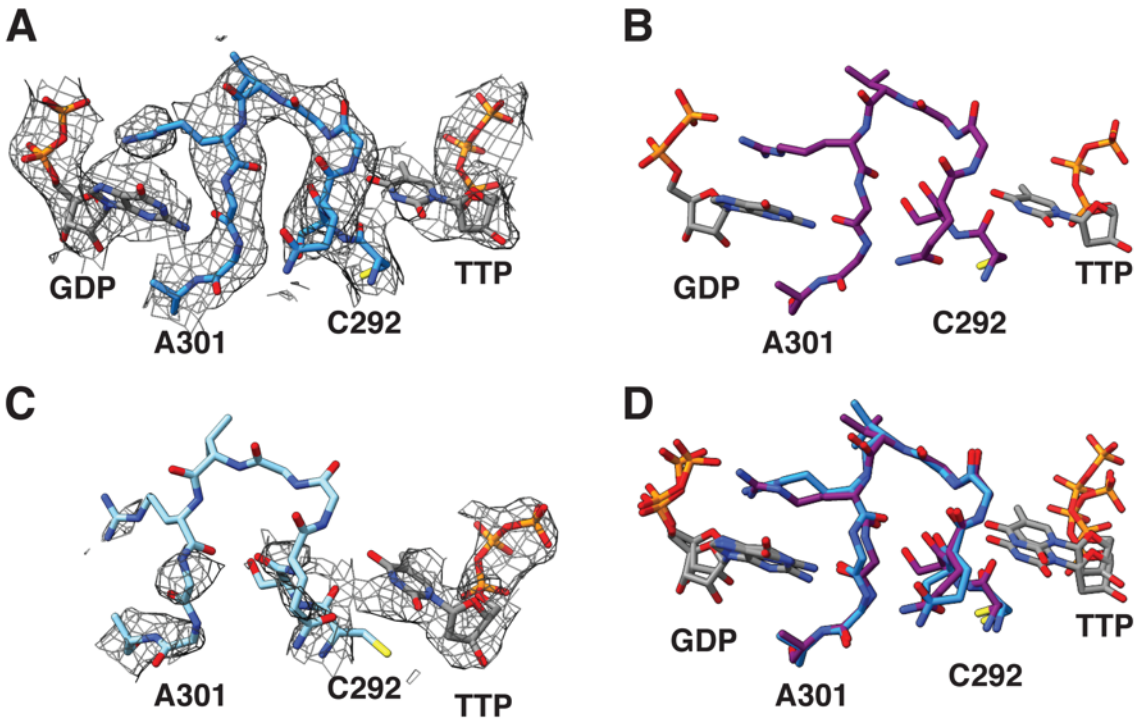

Fig. S8: Residues 292-301 in α, known as "loop 2" or the "specificity loop" in the RNR field, plays a key role in the communication between the specificity site and active site. A) This specificity loop in α is fully ordered. Nucleotide carbons shown in grey and protein carbons shown in blue. B) The specificity loop in the α4β4 crystal structure with GDP/TTP bound recapitulates contacts observed in panel A. Protein carbons shown in purple. C) The specificity loop in α′ is largely disordered. Protein carbons shown in light-blue. D) Overlay of panels A and B.

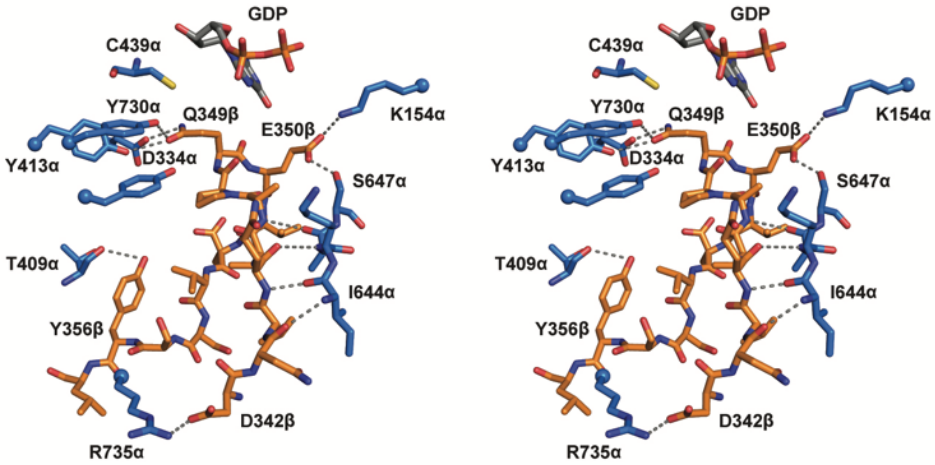

Fig. S9: Interactions between residues in the C-terminus of β and α. Distances less than 3.5 Å are highlighted in grey arrows and summarized in Table S2. Panels shown in wall-eye stereo.

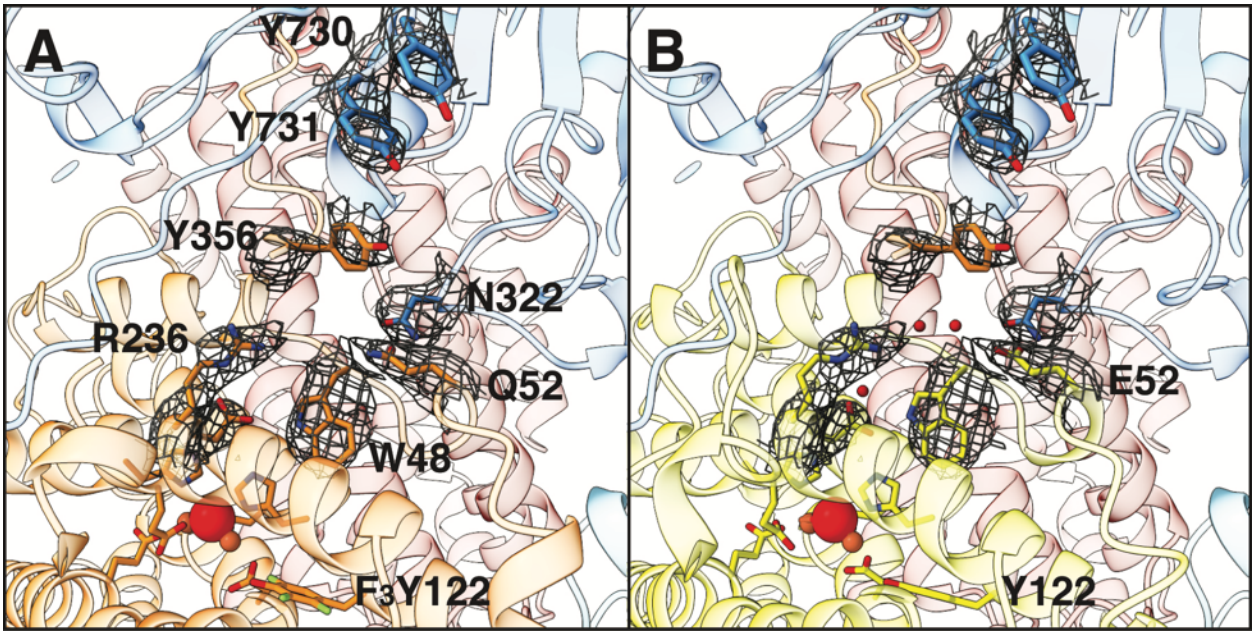

Fig. S10: E/Q52 is located at the α2-β2 interface A) Cryo-EM density supports the modeling of residues at the α2-β2 interface. Colors are as in Fig. 1. B) Superposition of a 2.05-Å resolution crystal structure of β2, where E52 is found in the same conformation (PDB 5CI4 (*32*), shown in yellow) as Q52β in our structure, shows that residue positions from crystal structure fit the cryo-EM density. The major difference between the β2 structure here and previous β2 structures is the ordering of the β-tail. The first 340 residues of our β2 structure align well with a previous 2.05-Å resolution crystal structure (*32*) of β2 with a root-mean-square deviation (RMSD) of 0.82 Å over 340 Cα atoms. Colors are as in Fig. 4. Density threshold set to 0.0262.

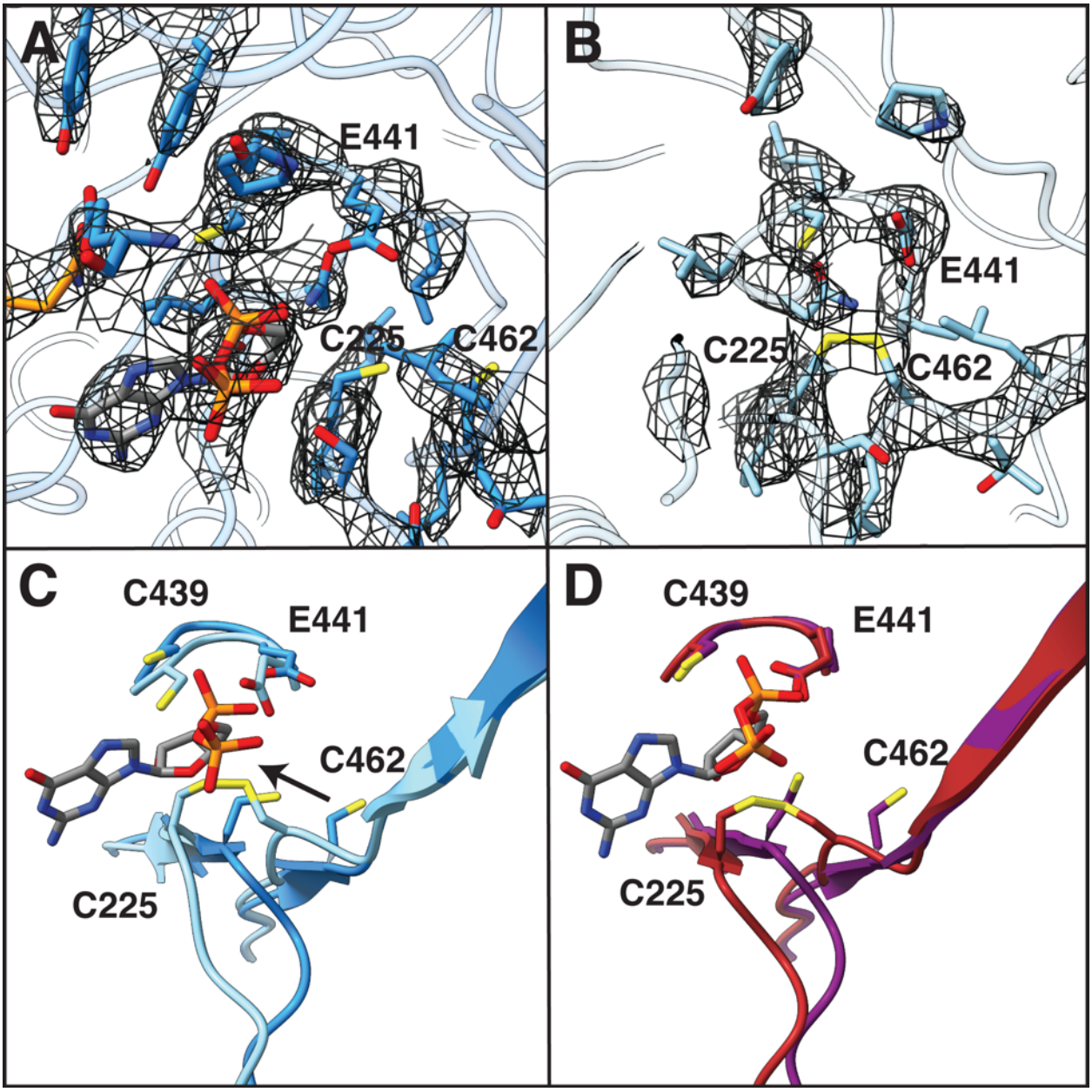

Fig. S11: The active site of α appears to be a pre-turnover state, with reduced cysteines C225 and C462 and with substrate bound whereas the active site of α′ appears to be a post-turnover state from which product has dissociated leaving behind a disulfide. A) Full view of α active site with density shown in mesh. Key residues are highlighted and GDP is shown in grey sticks. B) Full view of α′ active site with density shown in mesh and key residues highlighted. Density contoured to identical level as in Fig. 4. C) Overlay of active sites of α and α′ reproduced from main text figure 4C for comparison with panel D shown here. D) Overlay of previously reported crystal structures of α2 with reduced (purple, PDB: 5CNV (*13*)) and oxidized (brown, PDB: 2R1R (*14*)) active sites.

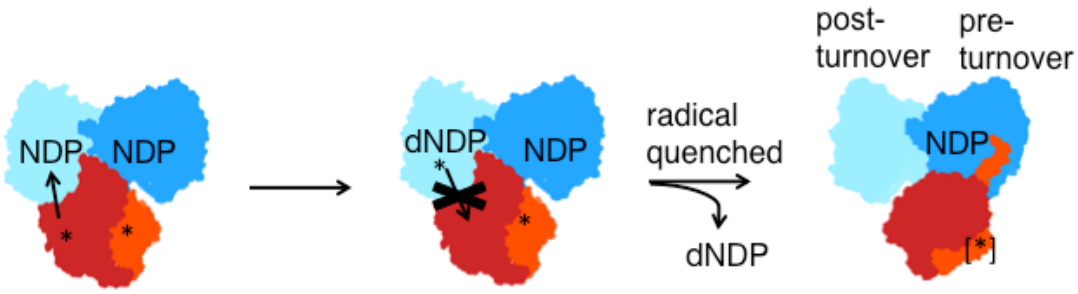

Fig. S12: Schematic for single turnover structural state trapped by cryo-EM in the presence of WT-α2 and E52Q/F_3Y122-β2. Left: Both monomers of α2 are primed with substrate (NDP) and effector and both monomers of β2 have a radical at F_3Y122. One radical fires and turnover occurs in the active site of α shown in light blue (α′). Middle: The radical is stalled on Y356. Product dissociates and β2 swings over to the other α monomer shown in darker blue (α). It is unclear whether F_3Y122 is re-oxidized prior to this shift. Right: The state trapped in our cryo-EM structure with one post-turnover state and one pre-turnover state. The fates of both radicals at this stage are not known.

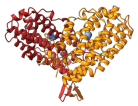

1990
Crystallography provides first structure of β2 (*E. coli*)
Nordlund et al *Nature (6)*

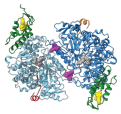

1994
Crystallography provides first structure of α2 (*E. coli*)
Uhlin and Eklund, *Nature (5)*

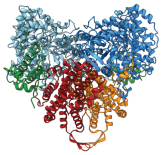

1994
Docking used to create the α2β2 "docking model" (*E. coli*) Uhlin and Eklund, *Nature (5)*

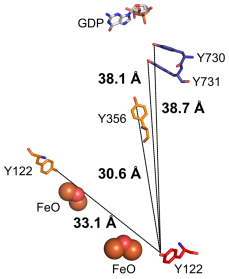

2005 - 2007
Spectroscopy provides multiple distances between PCET residues
Bennati et al *JACS (31)*
Seyedsayamdost et al *JACS (4)*

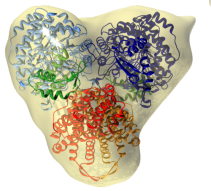

2011
Small-angle X-ray scattering used to generate a reconstruction of $\alpha_2\beta_2$ complex using WT *E. coli* class Ia proteins at
50 Å resolution
Ando et al *PNAS (8)*

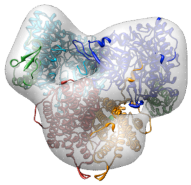

2013
Proof-of-principle that unnatural amino acids can be used to slow $\alpha_2\beta_2$ dissociation for structural studies by negative stain EM.
Structure at 32 Å resolution.
Minnihan et al *PNAS (7)*

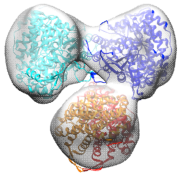

2017
Identification of the 2,3,5-fluorotyrosine122-E52Q-β construct used in this study to trap an active $\alpha_2\beta_2$ state
Lin et al *JBC (9)*
16 Å resolution negative stain model is unpublished

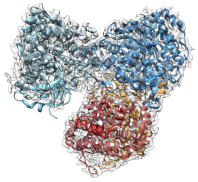

2020
Use of Cryo-EM and the 2,3,5-fluorotyrosine122-E52Q-β construct to generate a structure at 3.6 Å resolution
(this work)

Fig. S13: Schematic showing the application of biophysical methods and chemical biology tools in the interrogation of class Ia RNR from *E. coli*, the prototypic RNR. The structure presented here builds on decades of research from laboratories all over the world.

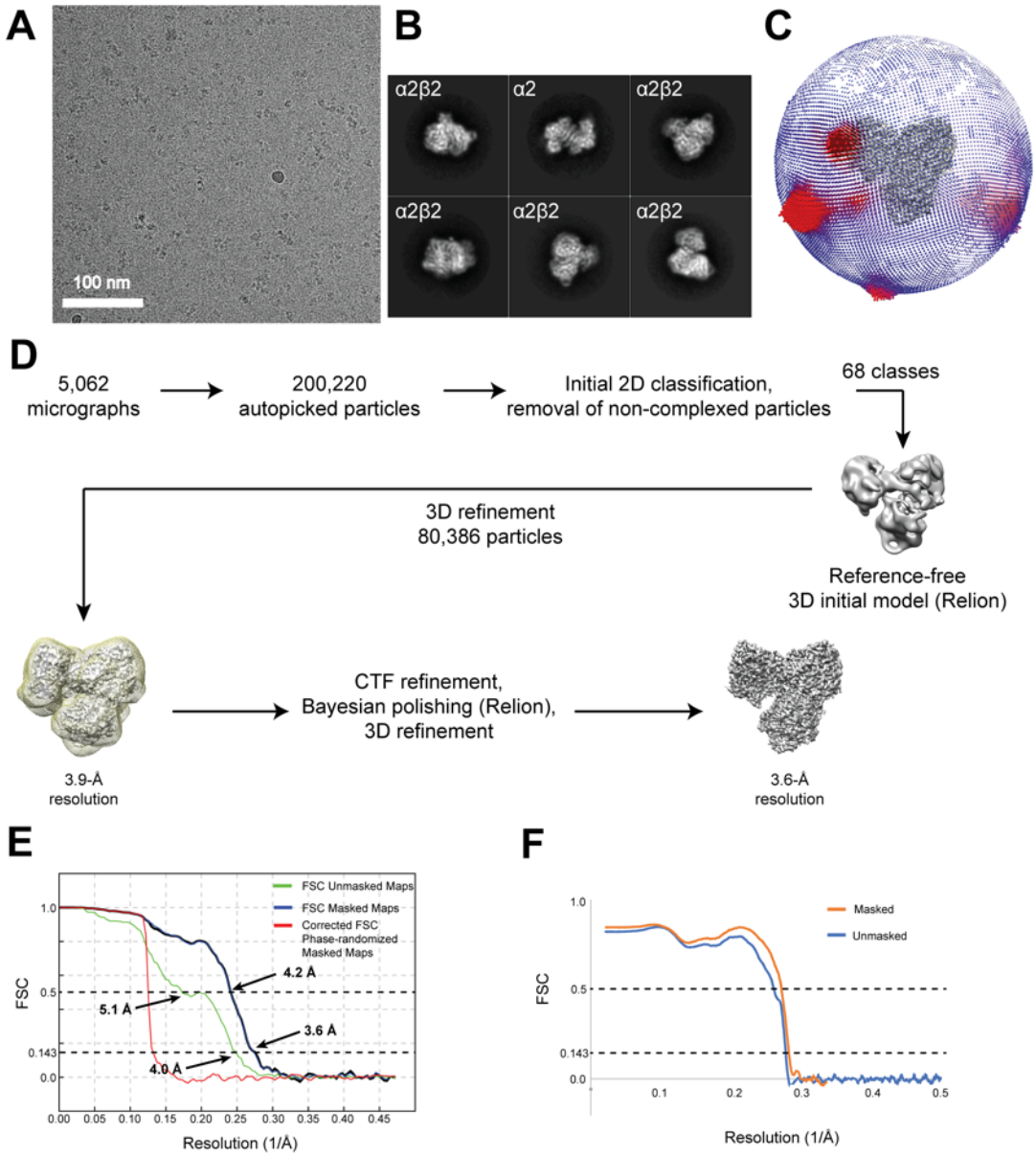

Fig. S14: Workflow of cryo-EM data processing. A) Representative micrograph with scalebar indicating 100 nm. B) Representative 2D class averages of α2β2, as well as uncomplexed α2, particles. C) Overlaid angular distribution plot from Relion (*38*) for the α2β2 complex. D) Workflow of data processing. 5062 micrographs were chosen based on initial CTF and drift assessment in SPHIRE (*36*) from an initial set of 6238 collected micrographs for further analysis. 200220 particles were autopicked using Topaz (*37*) and all subsequent analysis was performed using Relion 3.0 (*38*). E) FSC plots for unmasked (green) and masked (blue) maps for reconstruction shown in Fig. S14C. Resolution estimates at 0.5 and 0.143 FSC highlighted and shown. F) Map to atomic model FSC plots for both masked and unmasked maps, with dotted lines corresponding to 0.5 and 0.143 FSC.

Table S1. Predicted disordered regions based on lack of clear cryo-EM density

Chain	*Residues*
A (α′)	1-80
A (α′)	157-167
A (α′)	293-299
A (α′)	644-651
A (α′)	736-761
B (α)	743-761
D (β′)	342-375

Table S2. Distances less than or equal to 3.5 Å between key residues in β-C-terminus and in α

Residues	*Distance*
D342β – R735α	2.7 Å
N343β (backbone O) – I644α (backbone N)	3.1 Å
Q345β (backbone N) – I644α (backbone O)	3.2 Å
Q345β (backbone O) – A646α (backbone N)	3.5 Å
A347β (backbone N) – A646α (backbone O)	3.4 Å
Q349β – D334α	2.9 Å
Q349β – Y730α	3.3 Å
Q349β – Y413α	3.2 Å
E350β – K154α	3.0 Å
E350β – S647α	2.4 Å
Y356β – T409α (backbone carbonyl)	3.3 Å

Table S3. Imaging parameters and 3D Reconstruction

Microscope	FEI Titan Krios
Camera	Gatan K2
Acceleration voltage (kV)	300
Magnification (X)	130,000
Pixel size (Å)	1.059
Energy filter slit width	n/a
Defocus range (μm)	1.3-2.8
Number of frames	30
Exposure time (s)	6
Total exposure (e^- / Å)	47.1
Total micrographs collected	6238
Automation software	SerialEM
Particles Micrographs used for selection Windowed In final 3D reconstruction	 5062 200,220 80,386
Symmetry imposed	n/a (C1)
Map sharpening B-factor	-104.4
Estimated accuracy of rotations (°)	1.53
Estimated accuracy of translations (pix)	0.601
Unmasked resolution at 0.5/0.143 FSC (Å)	5.08/4.03
Masked resolution at 0.5/0.143 FSC (Å)	4.24/3.68
Local resolution range (Å)	3.3 – 5.5
EMDB accession code	EMD-21540

Table S4. Model refinement and validation

Number of atoms/residues/molecules	
Protein atoms, residues per chain	
Chain A	5854, 736
Chain B	5874, 738
Chain C	3061, 375
Chain D	2792, 341
Nucleotide atoms, molecules per chain	
Chain A	29, 1
Chain B	57, 2
Mg^{2+}	2
Fe	4
Water molecules	4
Secondary structure restraints	
Helices	102
Sheets	12
Ramachandran	2176
Hydrogen bonds	968
C-beta torsion restraints	4148
Ramachandran angles	
Favored (%)	94.03
Allowed (%)	5.97
Outliers (%)	0.05
r.m.s. deviations	
Bond lengths (Å)	0.004
Bond angles (°)	0.634
Molprobity	
Score	1.98
Clashscore	11.52
Omegalyze outliers (residues per chain)	0
B-factors (min/max/mean)	
Protein	31.76/206.25/73.37
Ligands	43.45/77.61/63.29
EMRinger Score	1.98
C-beta outliers (%)	0.00
CaBLAM outliers (%)	3.08
CC (mask)	0.77
PDB accession code	6W4X